Article:
Takaya, CA, Fletcher, LA, Singh, S et al. (2 more authors) (2016) Recovery of phosphate with chemically modified biochars. Journal of Environmental Chemical Engineering, 4 (1). pp. 1156-1165. ISSN 2213-3437

https://doi.org/10.1016/j.jece.2016.01.011

Recovery of phosphate with chemically modified biochars

C.A. Takaya[1], L.A. Fletcher[2], S. Singh[1], U.C. Okwuosa[1], A. B. Ross[1]*

[1]Energy Research Institute, School of Chemical and Process Engineering, University of Leeds; [2]School of Civil Engineering, University of Leeds, LS2 9JT, United Kingdom.

*Corresponding Author: A.B.Ross@leeds.ac.uk; Tel: +44(0)113 3431017

Highlights

- Biochar phosphate uptake can be enhanced from relatively low levels (e.g. 2.1% - 3.6%) to relatively high levels (66.4% - 70.3%) by impregnation with magnesium.
- Biomass pre-treatment with magnesium salts were markedly higher than those of biochar post-treatment.
- Biochar post-treatment with alkali also improved phosphate uptake capacity but was not a function of biochar surface area.

Abstract

The use of biochar for the recovery of phosphate has potential for environmental and socio-economic benefits but it is often characterised by relatively low nutrient adsorption capacity. The aim of this study was to investigate the potential for improving biochar phosphate adsorption capacities following chemical modification with metal salts, acids and alkali. Modified biochars were produced from oak wood and paprika waste (greenhouse waste) following either chemical treatment of biomass (in-situ modification) or biochar (post modification). Other chemical

treatments investigated included chemical oxidation, activation and salt treatment. Phosphate uptake capacities were determined by laboratory batch sorption tests, and results indicated that phosphate adsorption could be enhanced from relatively low levels (2.1% - 3.6%) to relatively high levels (66.4% - 70.3%) by impregnation with magnesium. These findings suggest that biochar mineral composition is a key property influencing biochar phosphate uptake capacity while surface area has less influence on sorption.

Key words: Biochar modification; Biomass pre-treatment; Phosphate sorption.

1. Introduction

Phosphates are essential plant nutrients but growing concerns about its future availability as well as its effects in water bodies (eutrophication) have made its recovery important (Rittmann et al. 2011; Wang et al. 2015a; Zeng et al. 2013). Recovery of phosphate is also necessary as it can be present at high concentrations in various agricultural and industrial wastewaters (Cai et al. 2013). Some studies have shown that biochars, the solid products formed from the thermochemical treatment of various kinds of organic matter, are capable of adsorbing various species including phosphates (PO_4-P) (Laird et al. 2010; Wang et al. 2015a; Yao 2013; Zeng et al., 2013; Zheng et al. 2010). Some studies have also reported that biochars are capable of releasing adsorbed PO_4-P, implying that such biochars could complement fertilizer use (Zheng et al. 2010). Nguyen et al. (2014) however observed that most agricultural by-products considered for environmental management including phosphate recovery require some form of modification. Indeed, there is growing interest in modifying biochar properties to enhance their adsorption capacities and other properties such

49 that “bespoke” or even smaller quantities of biochars are required for soil amendment
50 (Eberhardt et al. 2006; Novak et al. 2009; Silber et al. 2010; Wang et al. 2015a).

51 Ongoing research considers the development of waste-derived biochars with superior
52 sorption capacities and involves various treatment processes which can be broadly
53 categorised as liquid phase (chemical activation), gas phase (physical activation with
54 steam or carbon dioxide) or surface modification with chemicals, the lattermost not
55 always requiring a carbonisation step (Krishnan and Haridas 2008). Physical and
56 chemical activation treatments are more frequently employed, possibly because such
57 treatments offer greater improvements in char surface area and porosity development
58 due to the higher activation temperatures employed (T>450°C). Despite the lower
59 temperatures used in surface modification (60-80°C) however, comparable
60 improvements to surface area have been observed by Sricharoenchaikul et al. (2008).

61 Compared to physical activation, it has been suggested that chemical activation can
62 be cheaper, less time-consuming, and may provide more opportunities for char
63 porosity development (Krishnan and Haridas 2008; Lillo-Ródenas et al. 2003; Marsh
64 and Rodríguez-Reinoso 2006; Sricharoenchaikul et al. 2008). Moreover, in physical
65 activation, porosity development is achieved at the expense of carbon yield in some
66 cases (Viswanathan et al. 2009). Conversely, chemical agents within the carbon
67 feedstock might improve microporosity by interfering with the reduction in volume
68 which is known to occur as processing temperature increases, and by leaving behind
69 new pores when such agents are washed off (Marsh and Rodríguez-Reinoso 2006).
70 Consequently, chemical activation agents are frequently used, and include transition
71 metal salts, potassium and sodium hydroxides (Chen et al. 2011; Marsh and
72 Rodríguez-Reinoso 2006; Park et al. 2015). Other studies have focused on increasing
73 acidic surface functional groups via oxidation or acid treatment (Kastner et al. 2009;

74 Moreno-Castilla et al. 2000; Sricharoenchaikul et al. 2008; Xue et al. 2012), since
75 studies have shown that acidic and basic surface oxides are responsible for black
76 carbon cation and anion exchange properties respectively (Boehm 1994).

77 In terms of improving biochar properties for PO_4-P removal, studies have
78 demonstrated that the presence of basic oxygen functional groups such as metal
79 oxides, ketones, pyrones and chromens can improve biochar PO_4-P uptake (Chen et
80 al. 2011; Nyugen et al. 2012, 2014; Park et al. 2015; Wang et al. 2015a; Xue et al.
81 2009; Yao 2013; Zeng et al. 2013). Various processing temperatures, activating
82 agents and loading ratios have been employed, which understandably produce
83 adsorbents with different PO_4-P sorption capacities even when similar chemical
84 activation agents are used. For instance, while some studies have reported
85 improvements in adsorbent PO_4-P uptake following Fe-treatment (Krishnan and
86 Haridas 2008; Nyugen et al. 2013), about 51% decrease has been observed in other
87 studies (Yao 2013). This study was therefore aimed at contributing to growing
88 research on the optimal parameters required for obtaining biochars with superior PO_4-
89 P uptake hence improving their agronomical value. Consequently, the PO_4-P sorption
90 capacities of biochar derived from traditionally used biomass (oak) and agricultural
91 waste (paprika waste) with comparable carbon contents (>40%) were evaluated
92 following activation with various chemical agents to understand the effect of these
93 treatments on biochar PO_4-P recovery. Furthermore, the effect of treatment route (i.e.
94 biomass pre-treatment versus biochar post-treatment) was investigated for chemical
95 treatments which demonstrated the greatest improvements in biochar PO_4-P uptake.

96 ## 2. Methods

97 ### 2.1 Facilities

Biochars produced from holm oak were obtained from a commercial pyrolysis plant operated by Proininso (Spain) at 450 ℃ and 650 ℃ (designated OAK 450 and OAK 650 respectively). Biochar produced from greenhouse paprika waste possessing comparable carbon content to OAK 450 and OAK 650 was produced by the Energy research Centre of the Netherlands (ECN) at 400 ℃, and designated GHW 400.

2.2 Biochar and biomass treatment

All chemicals used for biochar and biomass treatment were of analytical grade and used as-received.

2.2.1 Chemical activation with metal chloride salts

Following a methodology similar to that of Zhang et al. (2012), 10 g oak biochars were mixed with 40 g $FeCl_3 \cdot 6H_2O$ in 60 mL distilled water iron chloride hexahydrate, stirred thoroughly and left to stand for 2 h at room temperature. The mixture was heated for 24 h at 100 ℃ on a Stuart hotplate before pyrolyzing biochar for 1 h in a nitrogen atmosphere at 5 mL min^{-1} and heating rate of 10℃ min^{-1} at 400 or 600 ℃ depending on the biochars' original production temperatures. That is, OAK 450 was pyrolyzed at 400 ℃ while OAK 650 was pyrolyzed at 600 ℃ to correspond with temperatures slightly below initial production temperatures. Modified biochars were subsequently rinsed with distilled water and oven dried at 100 ℃ for 2 h. This procedure was repeated for biochars treated with $MgCl_2 \cdot 6H_2O$ on oak biochars with particle size ≤ 850 µm, ≤2 mm and ≤4.75 mm.

Additional magnesium treatments were performed: to compare the effect of magnesium treatment route (in situ treatment versus biochar post-treatment), as-received holm oak chips and greenhouse waste biomass were treated with

$MgCl_2 \cdot 6H_2O$ as outlined above and pyrolyzed at 600 ºC. Secondly, to investigate the effect of pyrolysis temperature on magnesium loading onto already-made biochars, OAK 650 was pyrolyzed at 400 and 600 ℃ and stored for PO_4-P sorption analysis.

2.2.2 Surface and chemical activation with KOH

For surface activation, 4 g of biochar (particle size $\leq$2 mm) was mixed in a solution of 2 g KOH and 20 mL of distilled water. The mixture was stirred for 2 h at 75 ℃ with a magnetic stirrer. The treated biochars were subsequently rinsed with HCl followed by distilled water until the leachate pH values ranged between 6-7 then oven-dried for 2 hours at 100 ℃. This treatment was done for OAK 450, OAK 650 and GHW 400 biochars.

For chemical activation of oak biochars, the same procedure as outlined for surface modification was performed but with an additional pyrolysis step, where OAK 450 and OAK 650 were pyrolyzed for 1 h in a nitrogen atmosphere at 5 mL min^{-1} and heating rate of 10 ℃ min^{-1} at 400℃ and 600 ℃ respectively. Treated biochars were washed and dried as outlined above.

To compare the effect of KOH activation on raw biomass, 4 g holm oak and greenhouse waste were each soaked in 20 mL distilled water containing 2 g KOH followed by pyrolysis in nitrogen at 5mL min^{-1} at 600 ℃ for 1 h at a heating rate of about 10 ℃ min^{-1}. Biochars were rinsed with HCl followed by distilled water until the leachate pH values ranged between 6-7 and oven–dried for 2 h at 100 ℃.

2.2.3 Surface activation with H_2O_2

2 g biochars of particle size $\leq$2 mm were soaked in 20 mL of 10% and 30% H_2O_2 for 48 h at room temperature, using a methodology similar to that of Moreno-Castilla et

al. (2000) and Xue et al. (2012) without agitation, after which biochars were heated at 80 ℃ for 24 h, washed with distilled water until the pH was between 6-7 and oven dried.

2.3 Agronomical analyses

Ultimate analyses of biochar samples were determined using a CHN Elemental Analyser (Thermo Scientific Flash 2000). Proximate analysis was performed in a muffle furnace. Macro- and micro-nutrient content of the chars was determined after acid digestion of chars in concentrated nitric acid and analyzed by Inductively-coupled Plasma-Mass Spectroscopy (ICP/MS, Perkin Elmer ELAN DRC ICP-MS) (Perkin Elmer). pH measurements with a pH meter (Hach Lange) were made after 1:20 char/distilled water mixtures were shaken and allowed to stand for 2 h. Scanning Electron Microscopy (SEM) and Electron Dispersive X-ray Spectroscopy (EDS) was performed on biochars using a Carl Zeiss EVO MA15 SEM with Oxford Instruments AZtecEnergy EDX system. Brunauer-Emmett-Teller (BET) surface area and pore size distribution of treated and untreated biochars were determined by N_2 gas adsorption (Tristar 3000 Micromeritics) at -196 ºC after outgassing at 120℃ for 2 h. BET surface area was determined from linear fit adsorption data generated while pore volumes were determined using the t-plot model. Total pore volumes were obtained at relative N_2 pressures of 0.99. Spectral analysis was performed using an iS10 Nicolet Attenuated Total Reflectance Fourier Transform Infrared (ATR-FTIR) spectrophotometer, taking 64 scans over a range of 4000-400 cm^{-1} at a resolution of 4 cm^{-1}.

Cation exchange capacity (CEC) was determined using a method similar to that of Brewer (2012) and Yuan et al. (2011). 20 mL distilled water was added to 1 g of biochar and shaken at 160 rpm for 10 min each in a water shaker bath (SW23 Julabo GmbH) at room temperature and filtered through a Whatman Grade 1 filter paper. This was repeated four more times, discarding the leachates each time. Biochars were saturated with 10 mL of 1 M sodium acetate with pH adjusted to 7 using a few drops of glacial acetic acid, shaken at 160 rpm for 16 min and filtered. This was repeated twice more, discarding the leachates each time, after which biochars were rinsed with ethanol thrice for 8 min each at 160 rpm. Three additions of 1 M ammonium acetate at pH 7 were used to displace sodium cations by shaking at 160 rpm for 16 min, storing the leachates for subsequent analysis. Analyses were done in duplicate and the average values are reported. The concentration of displaced sodium cations were determined by Atomic Absorption Spectroscopy (AAS) of 10 mL aliquots of the final leachates following the addition of 10 mL 2000 ppm KCl as ionization-suppressant.

2.4 Phosphate sorption tests

As anaerobic digestion plants and other agricultural and industrial wastewaters are known to possess considerably high PO_4-P concentrations, about 125 mg P L^{-1} was used in this study to investigate biochar PO_4-P removal efficiency. A small number of biochars were also tested at 21.3 mg P L^{-1} for comparative purposes, as previous studies have often evaluated adsorbent performance at this concentration range.

2.4.1 Batch adsorption

All containers were acid washed in a 1 M HCl bath and rinsed with deionised water before use. 0.1 g biochar ($\leq$850 µm) was transferred to plastic Nalgene containers and 100 mL of phosphate solution prepared from potassium phosphate monobasic

was added after its pH was adjusted to 7 with NaOH. The containers were sealed tightly and the mixtures shaken at 160 rpm for 24 h in a water shaker bath (SW23 Julabo GmbH) at room temperature, after which 10 mL aliquots of each sample were filtered through 0.45 µm Sartorius Minisart syringe filters for Ion Chromatography analysis (Metrohm 850 Professional IC). Most analyses were done in duplicate and the average values reported. The concentrations of adsorbed ions were determined as:

$$q_e = (C_o - C_e)\frac{V}{M} \qquad (1)$$

Removal efficiency was determined as:

$$\%\ \text{Removal} = \frac{C_o - C_e}{C_o} \times 100 \qquad (2)$$

where C_o and C_e = initial and equilibrium liquid-phase phosphate adsorbate concentrations respectively (mg L^{-1}); V = volume of solution (L); M = mass of biochar sample used (g).

2.4.2 Desorption isotherms

Biochars which had previously undergone phosphate adsorption as outlined in **Section 2.4.1** were filtered through a Whatman Grade 1 filter paper and desorption was done by extracting phosphate from biochars using 0.01 M KCl solution. The mixture was shaken at 160 rpm for 24 h in a water shaker bath at room temperature. Analysis was carried out in duplicate, and 10 mL aliquots of each sample were taken

after 24 h then filtered through 0.45 µm Sartorius Minisart syringe filters for Ion Chromatography analysis.

2.4.3 Adsorption kinetics

To investigate possible phosphate adsorption mechanisms in biochars, a selection of biochars ($\leq$850 µm) were added to about 400 mg PO_4 L^{-1} solutions as done in **Section 2.4.1** but 10 mL aliquots of each sample were taken at 2.5, 5, 7.5, 10 and 24 h then filtered through 0.45 µm Sartorius Minisart syringe filters for Ion Chromatography analysis. Adsorbate concentrations withdrawn at intervals were determined using Equation (3):

$$q_t = (C_o - C_t)\frac{V}{M} \qquad (3)$$

where q_t = amount of PO_4^{3-} adsorbed (mg g^{-1}); C_o and C_t = liquid-phase adsorbate concentrations at initial conditions and at time t respectively (mg L^{-1}).

3. Results and discussion

3.1 As-received biochar physicochemical properties

Table 1 presents key biochar physicochemical properties prior to chemical treatment. Biochar carbon contents were >50% as mandated by the IBI (IBI, 2014) and both oak and GHW biochars were alkaline. Oak biochar ash contents were lower than greenhouse waste biochar (GHW 400) and consequently possessed less macro-

minerals compared to GHW 400. GHW 400 also had the highest CEC (**Fig. 1**), followed by OAK 650. The higher CEC of OAK 650 relative to OAK 450 is contrary to the trend observed in biochars, wherein lower temperature chars possess more oxygen functional groups (Wang et al. 2015b) hence higher CEC.

FTIR spectra are presented in **Fig. 2** for the 1800-600 cm^{-1} region as most band differences were observed in this region. The characteristic O-H stretching band around 3500-3200 cm^{-1} was absent in all biochars. Furthermore, the absence of bands at 3200 cm^{-1} suggested that the biochars did not possess furans (Keiluweit et al. 2010). In the 1800-600 cm^{-1} region, 4 bands were observed in all biochars: sharp peaks around 1714-1698 cm^{-1} attributable to C=O stretching of carbonyl groups (Pradhan and Sandle 1999; Wu et al. 2011); 1440 cm^{-1} likely corresponding to ketone stretching as observed in lignocellulosic materials (Keiluweit et al. 2010); 1400 cm^{-1} likely due to aromatic C=C stretching (Park et al. 2015); 875 cm^{-1} possibly due to out-of-plane bending vibrations for β-glucosidic linkages or for C-O groups, aldehydes and benzene derivatives (Krishnan and Haridas 2008; Sricharoenchaikul et al. 2008). Additional bands were also present in OAK 450 and GHW 400 biochars at 1610 cm^{-1}, attributable to aromatic C=C stretching or conjugated ketone and quinone C=O stretching vibrations (Keiluweit et al. 2010; Park et al. 2015). A band at 1583-1575 cm^{-1} resulting from conjugated C=O stretching vibrations of hemicellulose or aromatic rings (Krishnan and Haridas 2008; Sricharoenchaikul et al. 2008).

In terms of PO_4-P removal efficiency, the highest PO_4-P uptake was observed in OAK 650 followed by GHW 400 (**Fig. 3**). Maximum PO_4-P uptake was achieved before 24 h: after 5 h in oak biochars and even earlier in GHW 400, possibly because of the high initial PO_4-P concentrations used in this study. No PO_4-P was detected from both

biochar types following desorption tests, suggesting that PO_4-P was strongly bound to the char or that the extracting solution was inadequate.

3.2 Treated biochar physicochemical properties

As two types of chemical treatment were used to modify biochars, activating agents are prefixed with "SA" and "CA" to represent surface activation and chemical activation respectively, the latter treatment involving an additional pyrolysis step. Various chemical treatments understandably had variable effects on biochar functionality as outlined henceforth.

3.2.1 CEC and functional groups

Surface activation with KOH increased biochar CEC, with the highest improvement observed in SA-KOH GHW 400 (**Fig. 1**). Min et al. (2004) have also observed CEC improvements following surface modification with bases. CEC decreased following treatments involving further pyrolysis steps (CA-KOH) however. For instance, while SA-KOH treatment increased OAK 450 and OAK 650 CEC by about 82 and 56 $cmol_c$ kg^{-1} respectively, the reverse was observed in oak biochars after CA-KOH treatment.

It is uncertain whether the increase in GHW 400 CEC following SA-KOH treatment can be attributed to oxidation of the biochar surface resulting from the presence of K and O following Equation (4) as outlined in Viswanathan et al. (2009), because while potassium salt complexes are formed even without carbonization (Ehrburger et al. 1986; Lillo-Ródenas et al. 2003), Equation (4) might only occur at much higher temperatures (Ehrburger et al. 1986; Lillo-Ródenas et al., 2003; Viswanathan et al. 2009):

$$K_2O + C \rightarrow C-O-K + K \qquad (4)$$

280 It is more likely that CEC improvements may have resulted from an increase in
281 carbonyl groups. This hypothesis is based on the marked CEC increase observed in
282 SA-KOH treatment of GHW 400 compared to oak biochars, the former biochar
283 possessing more carbonyl groups as seen in **Fig. 2**(**c**) (1760-1665 cm^{-1} bands).
284 Mallampati and Valiyaveettil (2013) reported ester bond cleavage into hydroxyl groups
285 following NaOH treatment. Yakout (2015) also found that KOH treatment increased
286 biochar phenolic groups; such base treatment is said to increase char CEC (Han et al.
287 2005). SA-H_2O_2 treatment also improved CEC although not as greatly as surface
288 treatment with SA-KOH treatment. This increase was possibly due to the formation of
289 oxygen-containing species following acid-catalysed hydrolysis reactions (Lin et al.
290 2012; Marsh and Rodríguez-Reinoso 2006). FTIR spectra confirmed that some band
291 intensities increased following some surface activation treatments, notably the 1700
292 cm^{-1} and 1440 cm^{-1} bands in GHW 400 after SA-KOH treatment (**Fig. 2**(**c**)). SA-KOH
293 OAK 450 also possessed a marginally higher peak at 1585 cm^{-1} relative to untreated
294 OAK 450. These suggest an increase in C=O groups. Following H_2O_2 and Mg
295 treatment, absorbance intensities either had no marked effect on biochar functional
296 groups or decreased their intensities.

297

298 **3.2.2 Surface area**

299 SA-KOH treatment increased the surface area of GHW 400 by 55% while a drastic
300 decrease of >75% was observed in SA-KOH treated oak biochars. An increase in
301 GHW 400 surface area may have resulted from demineralization by KOH or HCl (the
302 latter introduced during the rinsing stage of the procedure), as is known to occur
303 following alkali or acid treatment of feedstocks (Mahmoud et al. 2012; Mukherjee 2003;

304 Yakout 2015). Demineralization from KOH action is more likely, since preliminary tests
305 showed that increasing KOH/biochar loading ratios whilst maintaining the same HCl
306 concentration improved surface areas in all 3 biochars. For instance, SA-KOH treated
307 OAK 650 at 1:1 and 5:1 loading ratios had a surface area of 59.3 m^2 g^{-1} and 67.8 m^2
308 g^{-1} respectively. The demineralization was possibly more pronounced in GHW 400
309 owing to its higher ash content, especially if such inorganics were more loosely bound
310 to its carbon structure than in oak biochars. Dislodgement of these inorganics would
311 consequently increase pore spaces, although more studies are required to confirm
312 this.

313 The decrease in oak biochar surface areas following SA-KOH treatment likely
314 occurred because surface activation was not followed by high temperature treatment.
315 This was validated by the fact that an additional pyrolysis step performed on OAK 650
316 increased its surface area to 344.3 m^2 g^{-1}. Yet a similar KOH surface activation
317 process on physic nut waste biochar without further heat treatment resulted in an
318 increase in surface area from about 200 m^2 g^{-1} to >500 m^2 g^{-1} in Sricharoenchaikul et
319 al. (2008). As this study was aimed at improving biochar PO_4-P removal efficiency
320 however, less emphasis was placed on increasing biochar surface area as it was
321 observed that high and low surface area biochars performed comparably. This was
322 further demonstrated by CA-KOH OAK 650 (i.e., OAK 650 pyrolyzed after KOH
323 treatment) whose higher surface area did not improve its PO_4-P removal efficiency (as
324 shown in **Section 3.3.3**).

325 Generally however, KOH treatment is known to significantly improve surface areas in
326 feedstock (Azargohar and Dalai 2008; Gu and Wang 2012; Sricharoenchaikul et al.
327 2008) owing to intercalation of K atoms within carbon lamella. This results in an
328 increase in char porosity following their removal in a rinsing step (Sricharoenchaikul

et al. 2008; Viswanathan et al. 2009) but such reactions may typically occur at high temperatures through the series of reactions outlined in Viswanathan et al. (2009). Indeed in terms of porosity development, while chars benefit from H_3PO_4 and $ZnCl_2$ treatment at temperatures of <450 ℃ and <500 ℃ respectively, KOH treatment requires higher activation temperatures (Marsh and Rodríguez-Reinoso 2006).

Following a similar trend to SA-KOH treatment, a 46% increase was observed in GHW 400 after SA-H_2O_2 treatment while oak biochar surface areas decreased (53.3% and 73.1% for OAK 450 and OAK 650 respectively) with even greater reduction following 30% H_2O_2 treatment. Pereira et al. (2003) and Pradhan and Sandle (1999) respectively reported a 12% and 9.2% reduction in surface area following surface activation of activated carbon with <10% and 30% H_2O_2. It is not unusual for char surface areas to decrease following chemical treatment due to pore wall collapse (Moreno-Castilla et al. 2000; Pereira et al. 2003; Pradhan and Sandle 1999) or blockage of micropores by newly formed surface oxygen groups (Pradhan and Sandle 1999). However, Xue et al. (2012) and Yakout (2015) respectively reported that peanut hull hydrochar and rice straw biochar treated with 10% and 30% H_2O_2 increased char surface area by 7.7% and 55.4%. It remains unclear why H_2O_2 surface treatment has such variable effects, and further investigations are required to confirm whether compositional differences in ash content are influential factors.

3.2.3 Carbon content

While a decrease in carbon content between 13-23% was observed in OAK 650, carbon contents of OAK 450 and GHW 450 increased following most SA and CA treatments as seen in **Table 2** due to a reduction in other elements. The increase in carbon content in OAK 450 and GHW 400 following SA-H_2O_2 was contrary to findings

353 of Xue et al. (2012). However, increases in hydrogen and oxygen content for all acid
354 treated biochars were observed, and this suggests the presence of stable carbon-
355 oxygen complexes and available activated sites (Guerrero et al. 2005). These findings
356 suggest that benefits can be derived from chemical treatment in terms of improved
357 CEC and in some cases surface area without a great deal of material loss.

358

359

360

361 **3.3 Influence of chemical treatment on biochar PO_4-P uptake**

362 **3.3.1 Chemical activation with magnesium**

363 Mg treatment of oak biochar resulted in much greater PO_4-P uptake, particularly
364 smaller particle size (≤850 µm) biochars. **Fig. 3(b)** shows that biochars treated with
365 magnesium salts adsorbed the highest PO_4-P, with Mg-OAK 650 adsorbing more PO_4-
366 P than Mg-OAK 450. To identify whether this was due to differences in biochar
367 properties or to temperature, the PO_4-P removal efficiencies of OAK 650 pyrolyzed at
368 400ºC and 600ºC were compared. PO_4-P sorption was found to be much lower in the
369 former suggesting that temperatures >400 ℃ are required for developing adequate
370 PO_4-P adsorbents. SEM/EDS of OAK 650 following Mg treatment at 600 ºC confirmed
371 the presence of Mg (**Fig. 4(a)**) while no visible differences were observed in OAK 450
372 ºC after 400 ℃ Mg treatment (data not included). Some Mg^{2+} was leached into the
373 PO_4-P solution during the test, as evidenced by the slightly lower count number seen
374 in **Fig. 4**(**b**) and from ion chromatography data (data not included).

375 As there was a marked improvement to PO_4-P uptake observed for 600 ℃ Mg
376 treatment, this temperature was used for Mg-treatment of unpyrolyzed oak and
377 greenhouse waste. Both Mg-treated biomass samples showed even greater PO_4-P
378 uptake compared to their Mg-treated biochar counterparts (**Fig. 3)** and compare
379 favourably with adsorbents from previous studies (**Table 3**). Thus in-situ magnesium
380 modification is more attractive than biochar post-treatment in terms of PO_4-P uptake
381 and cost, as a single-step modification and pyrolysis process is involved which
382 reduces energy requirements. Following desorption tests, 8.9 mg g^{-1} PO_4-P was
383 released from Mg-treated oak biomass, but was undetected in the case of greenhouse

384 waste biomass. Further investigations are required to better understand why PO_4-P
385 release was low, as this impacts its potential for use as a soil fertilizer, or for repeated
386 use in wastewater.

387 For both in-situ and post-treatment magnesium modification processes, coexisting
388 ions were not found to have an adverse effect on PO_4-P uptake: from a 450 mg L^{-1}
389 solution of NH_4^+ and PO_4^{3-}, oak chips pyrolysed following Mg treatment (in-situ
390 modification) recovered 66% and 72% PO_4-P at pH 7 and 8.5 respectively. This is
391 expected, given that pH ranges >7 are typically used for struvite precipitation.
392 Similarly, high PO_4-P removal efficiencies were maintained by in-situ modified
393 greenhouse waste and oak chips in synthetic wastewater (**Table 3**). Other studies
394 (Yao 2013; Zhang et al. 2009) similarly found that PO_4-P uptake was not greatly
395 affected by coexisting ions.

396 **3.3.2 Iron treatment**

397 Ferric chloride treatment performed on oak biochars resulted in only modest
398 improvements to PO_4-P removal efficiency. Yao (2013) found that surface modification
399 of biochars with iron nitrate decreased PO_4-P uptake from pure PO_4-P solutions (pH
400 7) by about 51%. Conversely, Krishnan and Haridas (2008) and Nyugen et al. (2013)
401 found that adsorbent treatment with iron nitrate and chloride salts improved PO_4-P
402 uptake from pure PO_4-P solutions (pH 3).

403 Three hypotheses may be drawn from these studies: Fe-treated adsorbents may
404 perform best in PO_4-P solutions with low pH; in other words, PO_4-P solution pH may
405 be more important than the nature of Fe salt used for adsorbent modification. This is
406 understandable given that anion exchange capacity is pH-dependent (Biswas et al.
407 2007; Zhang et al. 2009). While Wang et al. (2011) demonstrated that adsorbent

408 treatment with Fe^{2+} salt improved PO_4-P adsorption capacity to a greater extent than
409 with Fe^{3+} salt, maximum PO_4-P uptake was achieved at the lowest pH conditions for
410 both Fe^{2+} and Fe^{3+} treated adsorbents. Secondly, Fe treatment method may influence
411 adsorbent PO_4-P uptake. Nyugen et al. (2014) recommended the base treatment
412 (saponification) or oxidation of adsorbent materials prior to metal loading as evidence
413 suggests that such cationization processes improve the effectiveness of metal
414 deposition onto adsorbents, thus enhancing their PO_4-P removal efficiency. In one
415 study however (Carvalho et al. 2011), although adsorbent etherification prior to Fe^{2+}-
416 treatment improved adsorbent PO_4-P uptake, a comparable result was obtained by
417 non-etherified Fe^{2+}-treated adsorbent, with 97% and 93% removal efficiencies
418 respectively. Finally, it is reasonable for biomass or biochar composition to influence
419 the effectiveness of Fe treatment. From the few studies highlighted earlier however,
420 differences between high efficiency Fe-treated PO_4-P adsorbents (coir pith, sugarcane
421 bagasse, orange waste, activated carbon) and low efficiency Fe-treated adsorbents
422 (anaerobically digested sugar beet tailing biochar, oak biochar) are not readily
423 discernible. Yao (2013) however suggested that ferric hydroxide precipitates might
424 have coated biochar MgO (periclase), the latter likely being responsible for PO_4-P
425 uptake.

426 Overall, these findings suggest that surface activation of biochars with or without a
427 pre-treatment step is sufficient for improving adsorbent PO_4-P removal efficiency. pH
428 seems to influence Fe-loaded adsorbent PO_4-P removal efficiency to a larger extent
429 than adsorbent composition or treatment route. In other words, an additional pyrolysis
430 step following biochar treatment in Fe solutions may not be necessary.

431

3.3.3 KOH Treatment

SA-KOH treatment improved PO_4-P uptake by GHW 400, and previous studies (Samadi 2006; Sarkhot et al. 2013) have suggested ligand exchange between OH^- and PO_4^{3-}. Further studies are required however, as FTIR did not show much hydroxyl groups present in GHW 400 and most other chars in this study. Furthermore, preliminary PO_4-P sorption tests on SA-KOH treated oak biochars showed some improvement in their PO_4-P removal efficiencies, but were comparable to CA-KOH treated oak biochars. Low PO_4-P uptake following similar CA-KOH treatment was also observed elsewhere (Park et al. 2015).

3.3.4 H_2O_2 Treatment

Figs. 3(a)-(c) show that H_2O_2-treated OAK 450 and GHW 400 did not improve PO_4-P uptake. The decrease in PO_4-P uptake by such treated GHW 400 may be due to a reduction in magnesium and other inorganic elements as earlier suggested, but further analysis is required to confirm this. This lack of improvement following acid treatment has also been observed elsewhere (Park et al. 2015), and may be attributed to the formation of greater negative functional groups on biochar surfaces after acid treatment (Wang et al. 2015b), which may have been the cause of decreased biochar adsorption capacity for anionic species.

3.4 PO_4-P adsorption kinetics

PO_4-P adsorption kinetics of unmodified biochars and some surface and chemically treated biochars were determined using the frequently used pseudo-first order, pseudo-second order and intraparticle diffusion models (Equations 5-7) with parameters determined from models' plots:

Pseudo-first order model: $\log\left(q_e - q_t\right) = \log q_e - \frac{k_1}{2.303} t$ (5)

Linearized pseudo-second order model: $\frac{t}{q_t} = \frac{1}{q_e} t + \frac{t}{k_2 q_e^2}$ (6)

Intraparticle diffusion model: $q_t = k_i t^{0.5}$ (7)

where q_t and q_e = amount of PO_4-P adsorbed at time *t* and at equilibrium respectively (mg g^{-1}); k_1, K_2 and K_i = rate constants for pseudo-first order (min^{-1}), pseudo-second order (g mg^{-1} min^{-1}) and intra-particle diffusion (mg g^{-1} $min^{-0.5}$) models respectively (Ho and McKay 1998).

q_e values obtained from adsorption kinetics experiments were generally lower than batch adsorption q_e values and this may be due to some sample loss while taking solution aliquots periodically. Both pseudo-first order and intraparticle diffusion models gave very poor fits for most biochars compared to the linearized pseudo-second order model. R^2 values in the lattermost were higher and there was better agreement between experimental and calculated q_e values (**Table 4**). The pseudo-second order model has also been found to be a better fit for describing char dye sorption (Mahmoud et al. 2012). Intercept values were high in the intra-particle diffusion model and the regression plot not passing through the origin suggested that intra-particle diffusion was not a rate-controlling step (Cheung et al. 2007).

Conclusions

Effective phosphate recovery is important from environmental and socio-economic aspects as PO_4-P is present in many types of wastewaters. This study was aimed at

investigating the potential for improving biochar phosphate adsorption capacities following chemical activation of biochars (post-treatment) and biomass (in-situ treatment) with metal salts, KOH and acids. In some cases, chemical treatment at low temperatures has been shown to improve biochar functionality somewhat. In terms of improving PO_4-P removal efficiency, biochars treated with magnesium salts were found to have a significant enhancement on the levels of PO_4-P adsorbed while other chemical activation methods improved PO_4-P adsorption marginally. Specifically, results showed that while untreated biochars adsorbed 0-4.4% phosphate, the treatment of oak and greenhouse waste improved phosphate adsorption from 3.6% to 70.3% in oak biochars, and from 2.1% to 66.4% in greenhouse waste biochars which compare favourably with other adsorbents.

Overall, findings from this study suggest that it is possible to enhance biochar phosphate adsorption capacity by treatment of biochars or biochar precursors (raw feedstock) with inorganic chemicals, albeit with more process optimization. Further research is also required to better understand why adsorbed PO_4-P release was minimal for most biochars, as this determines biochars' potential for reuse or for soil amendment.

Acknowledgements

This study was funded by The Petroleum Technology Development Fund (PTDF) Nigeria, and the FERTIPLUS Consortium (Grant Agreement N°: 289853), co-funded by the European Commission, Directorate General for Research & Innovation, within the 7th Framework Programme of RTD, Theme 2 – Biotechnologies, Agriculture & Food. The views and opinions expressed in this study are purely those of the authors

and may not in any circumstances be regarded as stating an official position of the European Commission. The authors also wish to thank the technical staff of the Civil Engineering department and Energy Research Institute, University of Leeds, West Yorkshire, UK.

References

Azargohar, R., Dalai, A.K., 2008. Steam and KOH activation of biochar: Experimental and modeling studies. Microporous Mesoporous Mater. 110, 413–421. doi:10.1016/j.micromeso.2007.06.047

Biswas, B.K., Inoue, K., Ghimire, K.N., Ohta, S., Harada, H., Ohto, K., Kawakita, H., 2007. The adsorption of phosphate from an aquatic environment using metal-loaded orange waste. J. Colloid Interface Sci. 312, 214–23. doi:10.1016/j.jcis.2007.03.072

Boehm, H.P., 1994. Some aspects of the surface chemistry of carbon blacks and other carbons. Carbon N. Y. 32, 759–769. doi:10.1016/0008-6223(94)90031-0

Brewer, C.E., 2012. Biochar characterisation and engineering. http://lib.dr.iastate.edu/etd/12284/

Cai, T., Park, S.Y., Li, Y., 2013. Nutrient recovery from wastewater streams by microalgae: Status and prospects. Renew. Sustain. Energy Rev. 19, 360–369. doi:10.1016/j.rser.2012.11.030

Carvalho, W.S., Martins, D.F., Gomes, F.R., Leite, I.R., Gustavo da Silva, L., Ruggiero, R., Richter, E.M., 2011. Phosphate adsorption on chemically modified sugarcane bagasse fibres. Biomass and Bioenergy 35, 3913–3919. doi:10.1016/j.biombioe.2011.06.014

Chen, B., Chen, Z., Lv, S., 2011. A novel magnetic biochar efficiently sorbs organic pollutants and phosphate. Bioresour. Technol. 102, 716–23. doi:10.1016/j.biortech.2010.08.067

Cheung, W.H., Szeto, Y.S., McKay, G., 2007. Intraparticle diffusion processes during acid dye adsorption onto chitosan. Bioresour. Technol. 98, 2897–904. doi:10.1016/j.biortech.2006.09.045

Eberhardt, T.L., Min, S.-H., Han, J.S., 2006. Phosphate removal by refined aspen wood fiber treated with carboxymethyl cellulose and ferrous chloride. Bioresour. Technol. 97, 2371–6. doi:10.1016/j.biortech.2005.10.040

Ehrburger, P., Addoun, A., Addoun, F., Donnet, J.-B., 1986. Carbonization of coals in the presence of alkaline hydroxides and carbonates: Formation of activated carbons. Fuel 65, 1447–1449. doi:10.1016/0016-2361(86)90121-3

529 Gu, Z., Wang X., 2012. Carbon materials from high ash biochar: A nanostructure similar to activated graphene,
530 Amer. Transact. Eng. Appl. Sci. [online]. http://tuengr.com/ATEAS/V02/015-034.pdf
531 Guerrero, M., Ruiz, M.P., Alzueta, M.U., Bilbao, R., Millera, A., 2005. Pyrolysis of eucalyptus at
532 different heating rates: studies of char characterization and oxidative reactivity. J. Anal. Appl.
533 Pyrolysis 74, 307–314. doi:10.1016/j.jaap.2004.12.008
534 Han, J.S., Min, S., Kim, Y., 2005. Removal of phosphorus using AMD-treated lignocellulosic
535 feedstock. http://www.fpl.fs.fed.us/documnts/pdf2005/fpl_2005_han001.pdf
536 Ho, Y., McKay, G., 1998. Kinetic models for the sorption of dye from aqueous solution by wood. Trans
537 IChemE. 76:183-191. doi:10.1205/095758298529326
538 International Biochar Initiative (2014) Standardized product definition and product testing guidelines for biochar
539 that is used in soil http://www.biochar-
540 international.org/sites/default/files/IBI_Biochar_Standards_V2%200_final_2014.pdf
541 Kastner, J.R., Miller, J., Das, K.C., 2009. Pyrolysis conditions and ozone oxidation effects on
542 ammonia adsorption in biomass generated chars. J. Hazard. Mater. 164, 1420–7.
543 doi:10.1016/j.jhazmat.2008.09.051
544 Keiluweit, M., Nico, P.S., Johnson, M.G., Kleber, M., 2010. Dynamic molecular structure of plant
545 biomass-derived black carbon (biochar). Environ. Sci. Technol. 44, 1247–53.
546 doi:10.1021/es9031419
547 Krishnan, K.A., Haridas, A., 2008. Removal of phosphate from aqueous solutions and sewage using
548 natural and surface modified coir pith. J. Hazard. Mater. 152, 527–35.
549 doi:10.1016/j.jhazmat.2007.07.015
550 Laird, D., Fleming, P., Wang, B., Horton, R., Karlen, D., 2010. Biochar impact on nutrient leaching
551 from a Midwestern agricultural soil. Geoderma 158, 436–442.
552 doi:10.1016/j.geoderma.2010.05.012
553 Lillo-Ródenas, M.., Cazorla-Amorós, D., Linares-Solano, A., 2003. Understanding chemical reactions
554 between carbons and NaOH and KOH. Carbon N. Y. 41, 267–275. doi:10.1016/S0008-
555 6223(02)00279-8
556 Lin. Y., Munroe, P., Joseph, S., Henderson, R., Ziolkowski, A., 2012. Water extractable organic carbon in
557 untreated and chemical treated biochar. Chemosphere 87, 151-157. doi:10.1016/j.chemosphere.2011.12.007

558 Mahmoud, D.K., Salleh, M.A.M., Karim, W.A.W.A., Idris, A., Abidin, Z.Z., 2012. Batch adsorption of
559 basic dye using acid treated kenaf fibre char: Equilibrium, kinetic and thermodynamic studies.
560 Chem. Eng. J. 181-182, 449–457. doi:10.1016/j.cej.2011.11.116
561 Mallampati, R., Valiyaveettil, S., 2013. Apple peels--a versatile biomass for water purification? ACS
562 Appl. Mater. Interfaces 5, 4443–9. doi:10.1021/am400901e
563 Marsh H, Rodríguez-Reinoso F (2006) Activation processes (Chemical), In: Activated Carbon,
564 Elsevier Ltd, London. pp. 322-323, pp. 326-327, pp. 330-332, pp. 345-246.
565 Min, S.H., Han, J.S., Shin, E.W., Park, J.K., 2004. Improvement of cadmium ion removal by base
566 treatment of juniper fiber. Water Res. 38, 1289–95. doi:10.1016/j.watres.2003.11.016
567 Moreno-Castilla, C., López-Ramón, M.., Carrasco-Marín, F., 2000. Changes in surface chemistry of
568 activated carbons by wet oxidation. Carbon N. Y. 38, 1995–2001. doi:10.1016/S0008-
569 6223(00)00048-8
570 Mukherjee, S., 2003. Demineralization and Desulfurization of High-Sulfur Assam Coal with Alkali
571 Treatment. Energy & Fuels 17, 559–564. doi:10.1021/ef0201836
572 Nguyen, T.A.H., Ngo, H.H., Guo, W.S., Zhang, J., Liang, S., Lee, D.J., Nguyen, P.D., Bui, X.T., 2014.
573 Modification of agricultural waste/by-products for enhanced phosphate removal and recovery:
574 potential and obstacles. Bioresour. Technol. 169, 750–62. doi:10.1016/j.biortech.2014.07.047
575 Nguyen, T.A.H., Ngo, H.H., Guo, W.S., Zhang, J., Liang, S., Tung, K.L., 2013. Feasibility of iron
576 loaded “okara” for biosorption of phosphorous in aqueous solutions. Bioresour. Technol. 150,
577 42–9. doi:10.1016/j.biortech.2013.09.133
578 Novak, J.M., Lima, I,. Xing, B., Gaskin, J., Steiner,C., Das, K., Ahmedna, M., Rehrah, D., Watts, D.,
579 Busscher, W., Schomberg, H., 2009. Characterization of designer biochar produced at different
580 temperatures and their effects on a loamy sand. Annals of Environ. Sci. 3:195-206.
581 Park, J.H., Ok, Y.S., Kim, S.H., Cho, J.S., Heo, J.S., Delaune, R.D., Seo, D.C., 2015. Evaluation of
582 phosphorus adsorption capacity of sesame straw biochar on aqueous solution: influence of
583 activation methods and pyrolysis temperatures. Environ. Geochem. Health 37, 969–83.
584 doi:10.1007/s10653-015-9709-9
585 Pereira, M.F.R., Soares, S.F., Órfão, J.J.., Figueiredo, J.L., 2003. Adsorption of dyes on activated
586 carbons: influence of surface chemical groups. Carbon N. Y. 41, 811–821. doi:10.1016/S0008-
587 6223(02)00406-2

588 Pradhan, B.K., Sandle, N.K., 1999. Effect of different oxidizing agent treatments on the surface
589 properties of activated carbons. Carbon N. Y. 37, 1323–1332. doi:10.1016/S0008-
590 6223(98)00328-5
591 Rittmann, B.E., Mayer, B., Westerhoff, P., Edwards, M., 2011. Capturing the lost phosphorus.
592 Chemosphere 84, 846–853. doi:10.1016/j.chemosphere.2011.02.001
593 Samadi, A., 2010. Phosphorus Sorption Characteristics in Relation to Soil Properties in Some
594 Calcareous Soils of Western Azarbaijan Province. J. Agric. Sci. Technol. 8, 251–264.
595 Sarkhot, D. V, Ghezzehei, T.A., Berhe, A.A., 2013. Effectiveness of biochar for sorption of ammonium
596 and phosphate from dairy effluent. J. Environ. Qual. 42, 1545–54. doi:10.2134/jeq2012.0482
597 Sricharoenchaikul, V., Pechyen, C., Aht-ong, D., Atong, D., 2008. Preparation and Characterization of
598 Activated Carbon from the Pyrolysis of Physic Nut (Jatropha curcas L.) Waste †. Energy & Fuels
599 22, 31–37. doi:10.1021/ef700285u
600 Silber, A., Levkovitch, I., Graber, E.R., 2010. pH-dependent mineral release and surface properties of
601 cornstraw biochar: agronomic implications. Environ. Sci. Technol. 44, 9318–23.
602 doi:10.1021/es101283d
603 Viswanathan, B., Neel, P., Varadarajan, T., 2009. Methods of activation and specific applications of
604 carbon materials, National Centre for Catalysis Research, Department of Chemistry, Indian
605 Institute of Technology Madras, Chennai, India, p.17, p.19, p. 23. https://nccr.iitm.ac.in/e%20book-
606 Carbon%20Materials%20final.pdf
607 Wang, Z., Guo, H., Shen, F., Yang, G., Zhang, Y., Zeng, Y., Wang, L., Xiao, H., Deng, S., 2015a.
608 Biochar produced from oak sawdust by Lanthanum (La)-involved pyrolysis for adsorption of
609 ammonium (NH4+), nitrate (NO3−), and phosphate (PO43−). Chemosphere 119, 646–653.
610 doi:10.1016/j.chemosphere.2014.07.084
611 Wang, B., Lehmann, J., Hanley, K., Hestrin, R., Enders, A., 2015b. Adsorption and desorption of
612 ammonium by maple wood biochar as a function of oxidation and pH. Chemosphere 138, 120–
613 126. doi:10.1016/j.chemosphere.2015.05.062
614 Wang, Z., Nie, E., Li, J., Yang, M., Zhao, Y., Luo, X., Zheng, Z., 2011. Equilibrium and kinetics of
615 adsorption of phosphate onto iron-doped activated carbon. Environ. Sci. Pollut. Res. Int. 19,
616 2908–17. doi:10.1007/s11356-012-0799-y

Wu, W., Yang, M., Feng, Q., McGrouther, K., Wang, H., Lu, H., Chen, Y., 2012. Chemical characterization of rice straw-derived biochar for soil amendment. Biomass and Bioenergy 47, 268–276. doi:10.1016/j.biombioe.2012.09.034

Xue, Y., Gao, B., Yao, Y., Inyang, M., Zhang, M., Zimmerman, A.R., Ro, K.S., 2012. Hydrogen peroxide modification enhances the ability of biochar (hydrochar) produced from hydrothermal carbonization of peanut hull to remove aqueous heavy metals: Batch and column tests. Chem. Eng. J. 200-202, 673–680. doi:10.1016/j.cej.2012.06.116

Xue, Y., Hou, H., Zhu, S., 2009. Characteristics and mechanisms of phosphate adsorption onto basic oxygen furnace slag. J. Hazard. Mater. 162, 973–80. doi:10.1016/j.jhazmat.2008.05.131

Yakout, S.M., 2015. Monitoring the Changes of Chemical Properties of Rice Straw–Derived Biochars Modified by Different Oxidizing Agents and Their Adsorptive Performance for Organics. Bioremediat. J. 19, 171–182. doi:10.1080/10889868.2015.1029115

Yao, Y., 2013. Sorption of phosphate and other contaminants on biochar and its environmental implications (Thesis). http://ufdcimages.uflib.ufl.edu/UF/E0/04/54/09/00001/YAO_Y.pdf

Yuan, J.-H., Xu, R.-K., Zhang, H., 2011. The forms of alkalis in the biochar produced from crop residues at different temperatures. Bioresour. Technol. 102, 3488–97. doi:10.1016/j.biortech.2010.11.018

Zeng, Z., Zhang, S., Li, T., Zhao, F., He, Z., Zhao, H., Yang, X., Wang, H., Zhao, J., Rafiq, M.T., 2013. Sorption of ammonium and phosphate from aqueous solution by biochar derived from phytoremediation plants. J. Zhejiang Univ. Sci. B 14, 1152–61. doi:10.1631/jzus.B1300102

Zhang, G., Liu, H., Liu, R., Qu, J., 2009. Removal of phosphate from water by a Fe-Mn binary oxide adsorbent. J. Colloid Interface Sci. 335, 168–74. doi:10.1016/j.jcis.2009.03.019

Zhang, M., Gao, B., Yao, Y., Xue, Y., Inyang, M., 2012. Synthesis of porous MgO-biochar nanocomposites for removal of phosphate and nitrate from aqueous solutions. Chem. Eng. J. 210, 26–32. doi:10.1016/j.cej.2012.08.052

Zheng, W., Sharma, B.K., Rajagopalan, N., 2010. Using Biochar as a Soil Amendment for Sustainable Agriculture. Illinois Sustainable Technology Center University of Illinois, Urbana-Champaign. https://www.ideals.illinois.edu/bitstream/handle/2142/25503/Using%20Biochar%20as%20a%20Soil%20Amendment%20for%20Sustainable%20Agriculture-final%20report%20from%20Zheng.pdf?sequence=2 [1 January 2013].

Table 1. Physicochemical properties of untreated biochars

Property	OAK 450	OAK 650	GHW 400
C (%)	65.7	76.5	59.0
H (%)	2.7	1.4	2.9
N (%)	0.6	0.8	1.2
S (%)	0	0	0.3
O¶ (%)	31.0	21.3	36.6
H/C	0.4	0.2	0.5
O/C	0.4	0.2	0.5
Ash (%)	11.7	15.2	27.0
Moisture content (%)	29.3	14.3	2.5
Volatile matter (%)	21.1	11.8	25.0
Organic matter (%)	88.3	85.7	70.5
pH	9.9	10.3	10.6
BET surface area, N_2 (m^2 g^{-1})	180.0	280.0	1.3
Total pore volume (cm^3 g^{-1})	0.150	0.160	0.003
P (%)	0.2	0.2	0.4
K (%)	1.1	0.6	4.1
Ca (%)	4.4	5.0	3.6
Mg (%)	0.2	0.3	0.9
Na (%)	0.1	0.0	0.4

¶Oxygen content determined as difference between % C, H, N, S; elemental and mineral contents determined on dry basis (db).

Table 2. Elemental contents of some treated biochars

Biochar	C	H	N	S	O¶
OAK 450 treated with KOH	74.1	3.2	0.5	0.02	22.2
OAK 650 treated with KOH	59.5	3.1	0.5	0.03	36.9
GHW 400 (surface) treated with KOH	70.3	4.0	0.9	0.05	24.8
OAK 450 treated with H_2O_2	71.3	3.9	0.5	0.00	24.3
OAK 650 treated with H_2O_2	63.7	2.3	0.5	0.00	33.3
GHW 400 treated with H_2O_2	68.8	4.6	0.9	0.46	25.2
OAK 450 treated with $MgCl_2{\cdot}6H_2O$ at 400 ℃	57.1	2.6	3.6	0.00	36.7
OAK 650 treated with $MgCl_2{\cdot}6H_2O$ at 600 ℃	65.1	1.8	0.7	0.11	32.3
Raw oak treated with $MgCl_2{\cdot}6H_2O$ at 600 ℃	53.6	2.5	0.3	0.20	43.5
Raw GHW treated with $MgCl_2{\cdot}6H_2O$ at 600 ℃	43.4	1.6	0.9	0.00	54.1

Carbon, hydrogen, nitrogen and sulphur contents expressed as % dry basis (db) and oxygen determined by difference between % C, H, N and S from 100.

Table 3. PO_4-P removal efficiencies of some adsorbents

	Present study			
	PO_4-P adsorbed (C_o = 67 mg PO_4^{3-} L^{-1})		PO_4-P adsorbed (synthetic wastewater)#	
Adsorbent	%	mg g^{-1}	%	mg g^{-1}
Oak 450℃ biochar	1.5	1.0 ± 2.2	7.2	14.8 ± 0.6
Oak 650℃ biochar	1	0.7 ± 0.1	6.1	4.1 ± 0.7
GHW 400℃ biochar	0	-2.2 ± 0.2	0	-4.9
Mg oak biochar (in-situ)	95.9	64.6 ± 0.2	>95	>64
Mg GHW biochar (in-situ)	96.5	65.1 ± 1.3	>95	>64

	Previous studies	
	PO_4-P adsorbed (C_o = 61 mg L^{-1} PO_4-P)	Reference
La oak sawdust biochar (500ºC)	~33	Wang et al. (2015a)
Fe (II) sugarcane bagasse fibre	97§	Carvalho et al. (2011)
MgO sugarcane bagasse biochar	>35	Zhang et al. (2012)
MgO sugar beet tailing biochar	>65	Zhang et al. (2012)
Digested sugar beet tailing biochar	>70	Yao (2013)
Fe-Mn binary oxide	>95	Zhang et al. (2009)
Fe (II) activated carbon	~63 - 96§	Wang et al. (2012)

Synthetic wastewater concentrations (mg L^{-1}): SO_4^{2-}: 27.5 ± 0.5; NO_2^-: 46.4 ± 0.5; PO_4^{3-}: 67.4 ± 4.2; NO_3^-: 889.1 ± 7.3; Mg^{2+}: 28.6 ± 5.3; Ca^{2+}: 150.2 ± 0.6; Na^+: 318.7 ± 14.3; K^+: 513.5 ± 6.0; NH_4^+: 561.0 ± 5.4.
§Initial PO_4-P concentrations of 11-46 mg L^{-1}; n.d.: not detected, thus total PO_4-P uptake assumed, although Mg^{2+} present in synthetic wastewater may have contributed to PO_4-P removal.

Table 4. Biochar PO_4-P adsorption kinetics model parameters for some biochars

Biochar	$q_{e\ exp}$	Pseudo-first order					Pseudo-second order					Intraparticle diffusion		
		m	C	$q_{e\ cal}$	K_1	R^2	m	C	$q_{e\ cal}$	k_2	R^2	k_i	C	R^2
OAK 450	24.08	0.000	1.2194	16.57	0.000	0.365	0.04	-4.15	22.6	-0.0005	0.996	0.05	38.08	0.009
OAK 650	24.14	0.000	1.516	32.81	0.000	0.656	0.05	-5.70	22.2	-0.0004	0.995	-0.31	50.94	0.369
GHW 400	16.57	0.000	0.6229	4.20	-0.001	0.037	0.07	15.72	15.1	0.0003	0.651	-0.52	36.78	0.022
OAK450-K	17.19	0.001	0.1726	1.49	-0.002	0.461	0.06	-5.08	16.1	-0.0008	0.994	-0.09	29.93	0.037
OAK650-K	25.86	0.000	0.9216	8.35	0.000	0.224	0.05	0.11	21.2	0.0198	0.984	0.41	29.45	0.228
GHW400-K_s	21.54	0.001	0.6585	4.56	-0.001	0.217	0.05	0.11	21.2	0.0198	0.984	0.11	27.39	0.026
OAK450-M	16.88	0.001	-0.199	0.63	-0.002	0.778	0.06	-10.45	15.6	-0.0004	0.974	-0.14	37.25	0.059
OAK650-M	101.79	0.000	1.9663	92.53	0.000	0.354	0.01	0.77	108.7	0.0001	0.991	4.21	22.97	0.856
OAK450-FC	16.56	0.003	0.7119	5.15	-0.007	0.399	0.06	-4.17	16.0	-0.0009	0.991	0.22	20.16	0.293
OAK650-FC	24.96	0.001	0.444	2.78	-0.001	0.768	0.04	-5.10	23.4	-0.0004	0.990	0.10	40.51	0.065

$Q_{e\ exp}$ and $Q_{e\ cal}$ = PO_4-P adsorbed determined from experiments and plots respectively (mg g^{-1}); k_1 (min^{-1}), k_2 (min g mg^{-1}) and K_i (mg g^{-1} $min^{-0.5}$) obtained from the respective plots of $\log(q_e-q_t)$ versus t, $\frac{t}{q_t}$ versus t and q_t versus $t^{0.5}$; suffixes K and K_s refer to biochar treatment with KOH (chemical activation for oak biochars and surface activation for GHW); suffixes M and FC refer to chemical activation with $MgCl_2{\cdot}6H_2O$ and $FeCl_3{\cdot}6H_2O$ respectively.

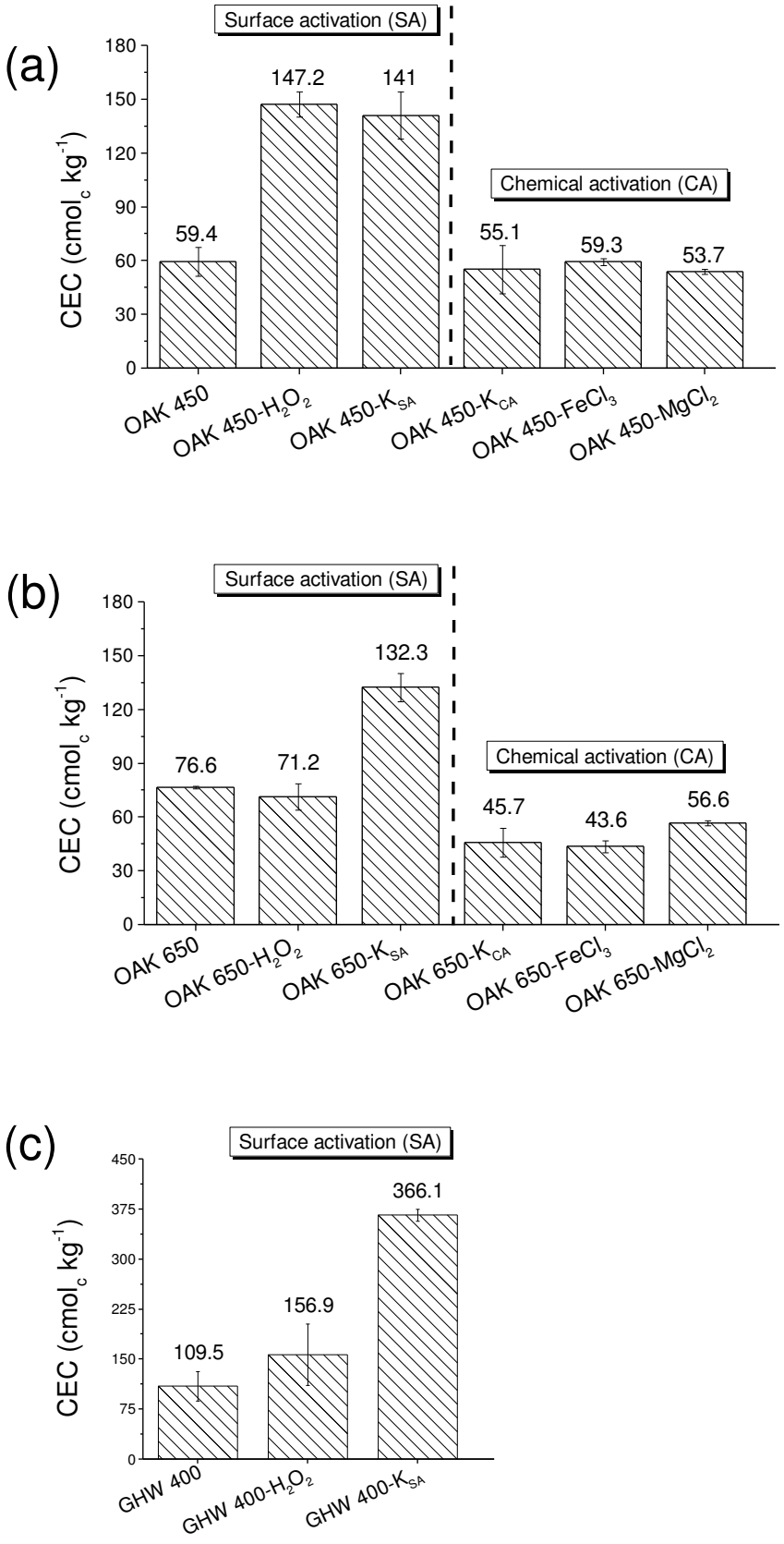

Figure 1. CEC values of some treated and untreated biochars

Surface activation with: KOH (K_{SA}), H_2O_2; chemical activation involving pyrolysis with: $FeCl_3 \cdot 6H_2O$ (FC), KOH (K_{CA}) and $MgCl_2 \cdot 6H_2O$

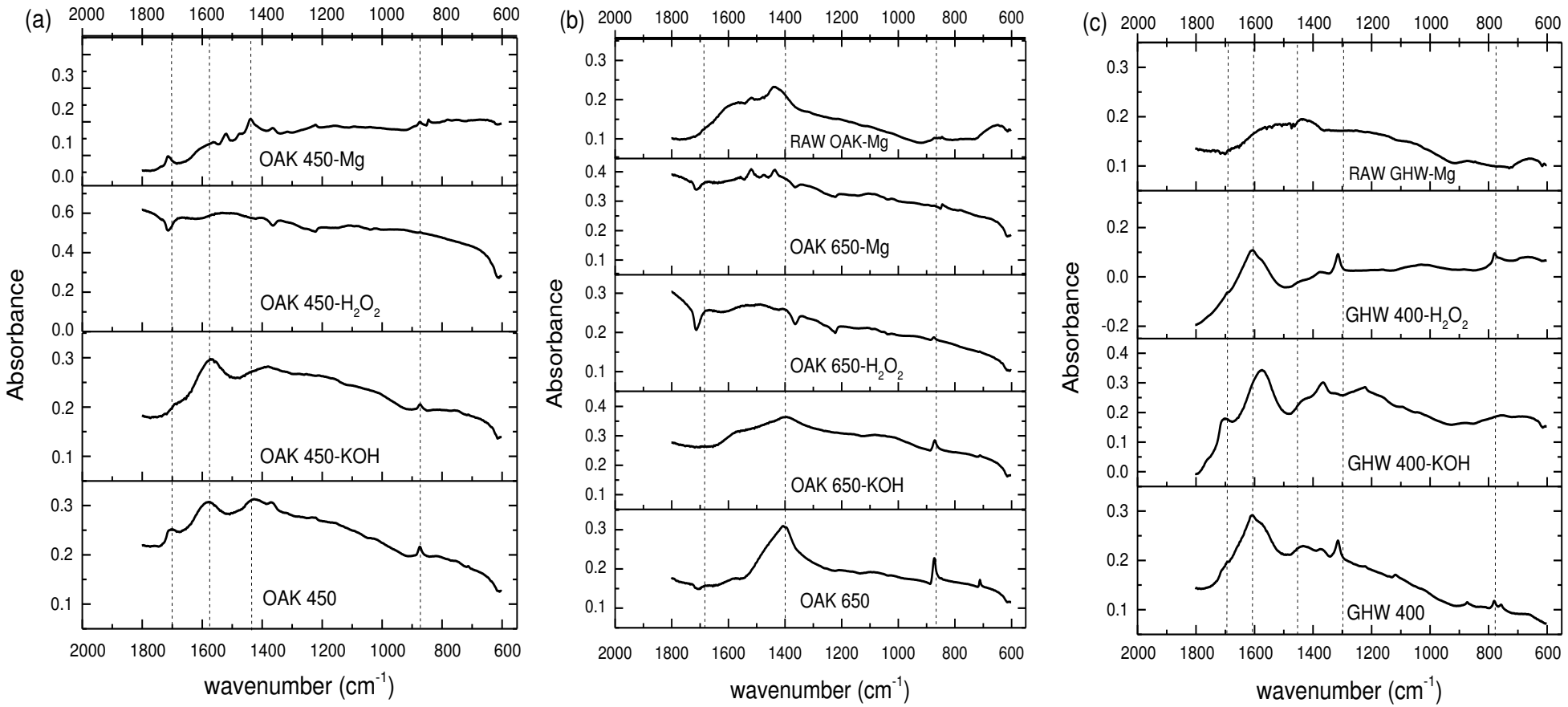

Figure 2. FTIR spectra of treated and untreated (a) OAK 450 (b) OAK 650 (c) GHW 400 biochars (K: KOH surface activation; H: H_2O_2 surface activation; Mg: chemical activation with $MgCl_2 \cdot 6H_2O$

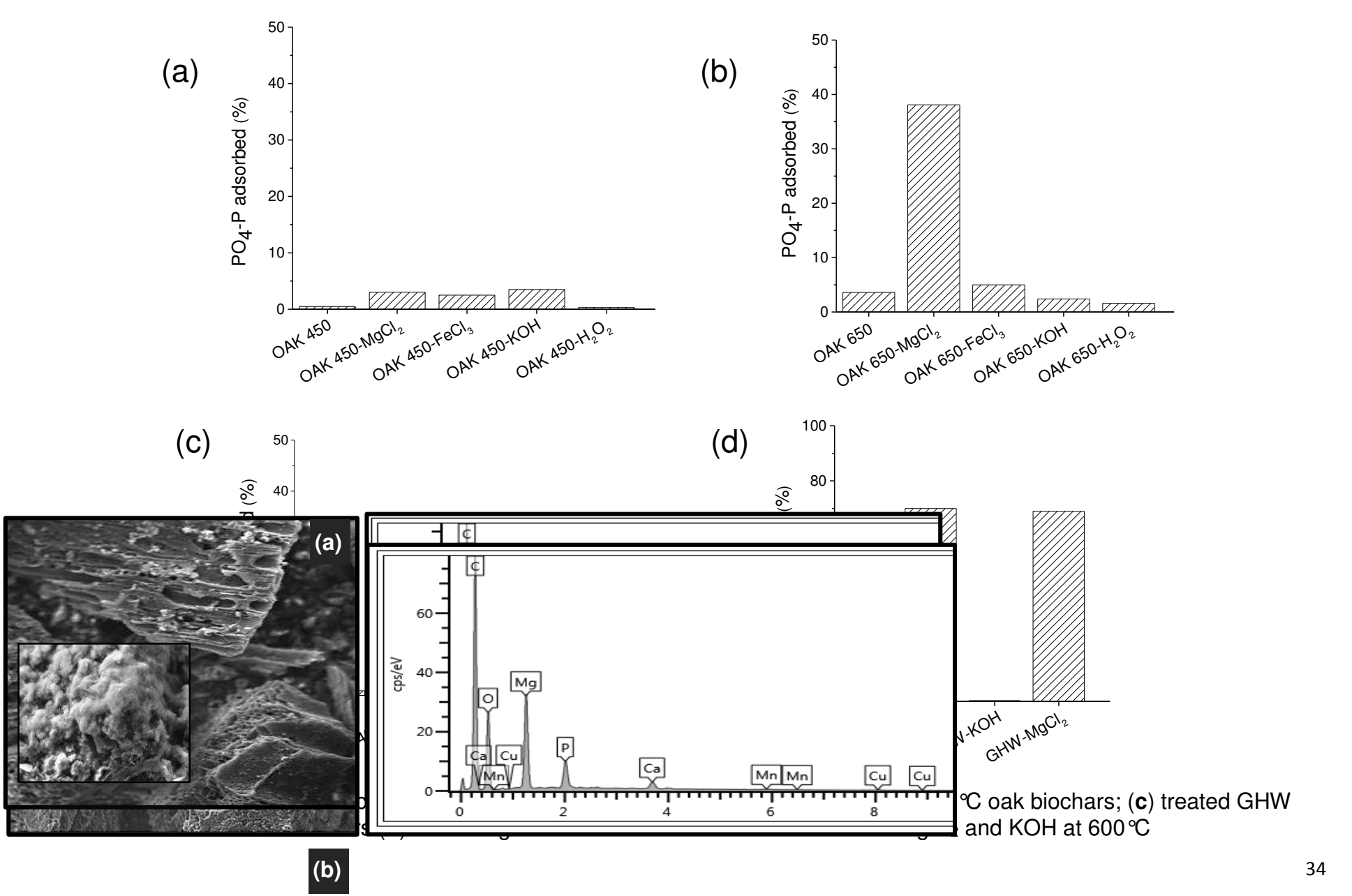

℃ oak biochars; (**c**) treated GHW
and KOH at 600℃

12

13